ISSN 1063-7842, Technical Physics, 2017, Vol. 62, No. 9, pp. 1398–1402. © Pleiades Publishing, Ltd., 2017.
Original Russian Text © M.V. Dorokhin, A.V. Zdoroveyshchev, E.I. Malysheva, Yu.A. Danilov, 2017, published in Zhurnal Tekhnicheskoi Fiziki, 2017, Vol. 87, No. 9, pp. 1389–1394.

PHYSICS
OF NANOSTRUCTURES

Heterostructures with InGaAs/GaAs Quantum Dots Doped by Transition Elements. Part I: Photoluminescence Properties

M. V. Dorokhin*, A. V. Zdoroveyshchev, E. I. Malysheva, and Yu. A. Danilov

Research Physicotechnical Institute, Lobachevsky Nizhny Novgorod State University, pr. Gagarina 23, Nizhny Novgorod, 603950 Russia

**email: dorokhin@nifti.unn.ru*

Received July 12, 2016

Abstract—The optical properties of InGaAs/GaAs quantum dot heterostructures that are doped by manganese and chromium during growth by Metal-organic vapor phase epitaxy have been studied. Surface topography photoluminescence spectra measurements have demonstrated the possibility of controlling the spectral characteristics of the structure by varying quantum well growth conditions and sizes in the presence of impurity atoms. Research results are explained by the peculiarities of InAs nanoclusters formation on the GaAs surface in the presence of Mn and Cr atoms.

DOI: 10.1134/S1063784217090055

INTRODUCTION

Over the last 20 years, light-emitting diodes (LEDs) based on InAs/GaAs quantum dot (QD) heterostructures have not only been the subject of basic research but also have been extensively used in commercial applications [1–5]. Specifically, the creation of QD-based lasers and LEDs operating at wavelengths of 1.30–1.55 μm, which are promising for fiberoptic communication, has been reported [1, 4–6]. The main advantages of QD structures are a deep confining potential and, in the long term, a narrow luminescence line (since the spectrum of a single QD is similar to that of an atom).

The most popular methods of QD formation use the effect of self-organization of nanoclusters during heteroepitaxy on a semiconductor with a differing lattice parameter [3, 4]. The main advantage of this approach is simplicity, whereas its disadvantage is the large distribution of the QD sizes in a QD array. As a result, the energy levels in single QDs shift with respect to each other [7] and the luminescence line broadens. To stabilize the QD growth surface and reduce their size dispersion, the material is doped by different impurities. The influence of doping on QD self-organization has been studied in a number of works [8–11]. By modifying the QD growth mechanism, one can controllably change the properties of QDs. For example, it was found that doping of QDs by bismuth during growth [8] changes the self-organization mechanism and causes the formation of an array of QDs with a narrower spectral line. Doping by manganese atoms [10, 11] is used to impart ferromagnetism to a QD array.

In the first part of this work, we report research data for InAs/GaAs QD heterostructures doped by Mn or Cr atoms in the course of QD formation. In spintronic devices, these impurities are used to control the charge carrier spin in Mn(Cr)-doped QDs. Unlike structures prepared in [10–12], those studied in this work were made by vapor-phase epitaxy [9, 13]. The aim of the investigation was to shed light on the QD formation mechanism in the presence of transition element atoms and find ways to controllably vary the properties of QD structures prepared by MOS hydride epitaxy. It has been shown that, by varying the impurity concentration, one can control the luminescence wavelength of the structures and extend the spectral range toward 0.9–1.3 μm.

1. EPITAXIAL METHODS

The structures were grown on (100) *n*-GaAs substrates by the method of vapor-phase epitaxy from metalorganic compounds and arsine at atmospheric pressure of carrier gas (hydrogen). First, a Si-doped *n*-GaAs (*n*-GaAs : Si) buffer layer and a thin (50 nm) layer of undoped GaAs were deposited at 650°C. Following that, the growth temperature was decreased to 520°C and an array of self-organized InAs QDs was deposited on the surface of the structure. The QDs were fabricated by the standard technology described in [9, 13, 14]. In the process of growth, the QDs were doped by Mn or Cr. Doping was carried out by sputtering a Mn(Cr) target using a pulsed Nd : YAG laser. The impurity concentration was varied by controlling the laser intensity. The concentration was estimated by comparing with identically grown reference struc-

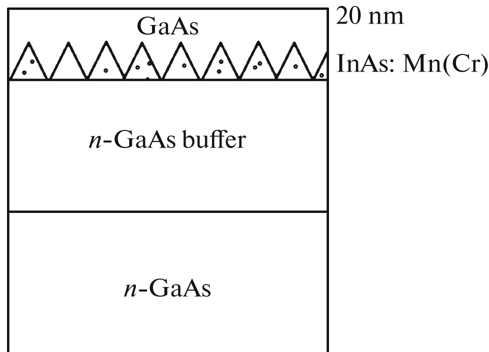

Fig. 1. Investigated structures with InAs : Cr and InAs : Mn QDs.

tures, which contained a single Mn delta-layer in GaAs. The sheet concentrations of Mn and Cr were found to fall into the interval 4×10^{12}–2×10^{13} cm^{-2} and (2–8) × 10^{13} cm^{-2}, respectively. After the formation of QDs, a thin (20 nm) undoped GaAs overlayer was grown on the surface. The overlayer was grown at the same temperature as the QDs. To be definite, QD : Mn and QD : Cr structures will be referred to as structure A and structures B, respectively. In addition, references structures (structures R) free of magnetic impurities near QDs were prepared.

The spectral behavior of the QD structures were studied by the method of photoluminescence (PL) spectroscopy at 77 K. Photoluminescence was excited by a 40-mW He–Ne laser. The morphology of the InAs QD array, which was visualized by the selective etching of the cap layer [15, 16], was examined by an NT-MDT Solver Pro atomic force microscope (AFM). The cap layer was etched in a selective etcher with an etching rate of 30 nm/min for GaAs and less than 1 nm/min for InAs. At $x = 0.2$, the etching of the $In_xGa_{1-x}As$ solid solution slowed down. Therefore, after the cap layer was all etched off, we observed the surface of the $In_xGa_{1-x}As$ layer with $x = 0.2$ (the threshold value of the composition). This technique was described in detail elsewhere [15, 16]. Tests specimens are shown in Fig. 1, and their parameters are listed in the Table 1.

Table 1. Parameters of test specimens. $Q_{Mn(Cr)}$ stands for the nominal concentration on Mn(Cr)

Structure	$Q_{Mn(Cr)}$, cm^{-2}	Expected type of conductivity
A1	4×10^{12}	Hole [10, 11, 13]
A2	8×10^{12}	Hole [10, 11, 13]
A3	2×10^{13}	Hole [10, 11, 13]
B1	2×10^{13}	High resistivity [12]
B2	4×10^{13}	High resistivity [12]
B3	8×10^{13}	High resistivity [12]
R	0	N/a

2. RESULTS AND DISCUSSION

2.1. Photoluminescence and Surface Morphology of Mn-Doped Structures (Structures A)

The PL spectra of structures A measured at 77 K are shown in Fig. 2. A wide band with a peak at about 1.2 eV, which is assigned to PL from the *n*-GaAs substrate was subtracted from all the spectra. PL spectrum measured of the undoped reference structure shows a band with a peak near 1 eV, which is associated with radiative transitions between states in QDs (Fig. 2, structure R). It was assumed [2] that this band is due to recombination in the QD array and its width correlates with the QD size distribution. Doping by manganese with a minimal sheet concentration of 4×10^{12} cm^{-2} changes the spectra; the total PL intensity grows and a second PL band (II) appears with a peak near 1.04 eV (Fig. 2, curve *1*). The spectral lines were analyzed by decomposing the experimental spectrum into Gaussian components. The second-to-first line intensity ratio is ~0.62 ± 0.05. The second PL peak may be assigned to radiative transitions in the array of QDs with sizes other than those in the first array. According to [15], both arrays may simultaneously exist in the spectrum even in the absence of manganese. When the Mn content grows to 8×10^{12} cm^{-2} (Fig. 2, curve *2*), the same tendencies are observed: the total PL intensity rises, and the third (III) and fourth (IV) bands arise at 1.16 and ~1.4 eV. Now the second-to-first line intensity ratio equals 0.61 ± 0.05 (that is, remains the same within an experimental error). When the sheet concentration of manganese, which is introduced into the QD area, equals 2×10^{13} cm^{-2}, the PL spectra of the structures change considerably (Fig. 2, curve *3*): the intensities of the lines that correspond to radiative transitions in the QD array markedly drop (below the spectral intensity for the reference structure). The highest intensity with a maximum near 1.4 eV is observed for band IV. The origin of this maximum is ambiguous. In the given energy interval, radiation sources are InGaAs QDs [17], separate Mn levels in GaAs [17, 18], and a wetting layer that arises during the growth of InAs QDs [15]. It is likely that, in the given case, radiation comes from the wetting InAs layer. It can be supposed that this layer is highly inhomogeneous because of the In diffusion into the GaAs substrate in the presence of Mn, as indicated by a wide PL line (37 meV). In this case, the total PL intensity drops to the PL intensity observed for the undoped reference structure. The PL data can be checked against the surface morphology data for the visualized QD array [15, 16] (Figs. 3a–3c). When studying the surface morphology of the undoped reference structure under the AFM, we revealed a QD array with the following mean parameters: a lateral size of ~60 nm, a

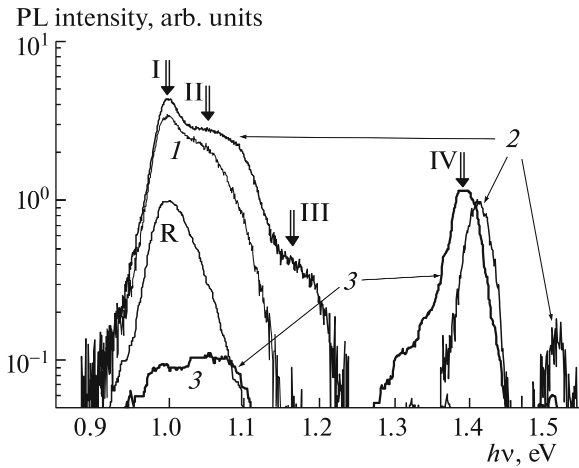

Fig. 2. PL spectra measured for InAs : Mn QDs at 77 K. The Mn content is (*1*) 4×10^{12}, (*2*) 8×10^{12}, and (*3*) 2×10^{13} cm^{-2}. Curve R is the spectrum of the reference structure. Roman numerals are the numbers of the PL peaks (see the text).

sheet concentration of 5×10^9 cm^{-2}, and a height of ~2.5 nm (Fig. 3a). It seems that clusters that are present in the AFM images are responsible for luminescence line I observed in the PL spectrum at 1 eV. In the structures that contain arrays of Mn-doped InAs QDs with a sheet concentration of 8×10^{12} cm^{-2}, the QD mean lateral size in an array of visualized QDs increases to about 90 nm (the increase exceeds the experimental error), the sheet concentration decreases to about 2×10^9 cm^{-2}, and the QD height decreases to about 2 nm (Fig. 3b). In the structures with a Mn concentration of 2×10^{13} cm^{-2} (Fig. 3c), QD arrays were absent: instead, a rather flat surface with a roughness mean height of about 0.5 nm was observed. This pattern is characteristic of, e.g., the visualized surface of an InGaAs QD.

The surface topography and PL data may be explained by the influence of Mn atoms on the formation of QDs. Mn atoms present on the surface change the thermodynamic conditions for nanoclustering, specifically, the surface energy and the surface diffusion length of atoms [13]. As a result, the nanocluster equilibrium size distribution also changes. For the reference structure, this function can be described by a Gaussian curve with a maximum that corresponds to the QD mean size in the array. Doping by manganese changes the Gaussian parameters (the mean size and distribution width) and, accordingly, the PL spectra (Fig. 2); i.e., additional spectral lines appear due to radiative transitions in the clusters with other equilibrium parameters (these clusters are seen in the AFM micrographs, Fig. 3b).

When the manganese content equals 2×10^{13} cm^{-2}, the concentration of nanoclusters responsible for luminescence in the energy range 1.0–1.3 eV seems to

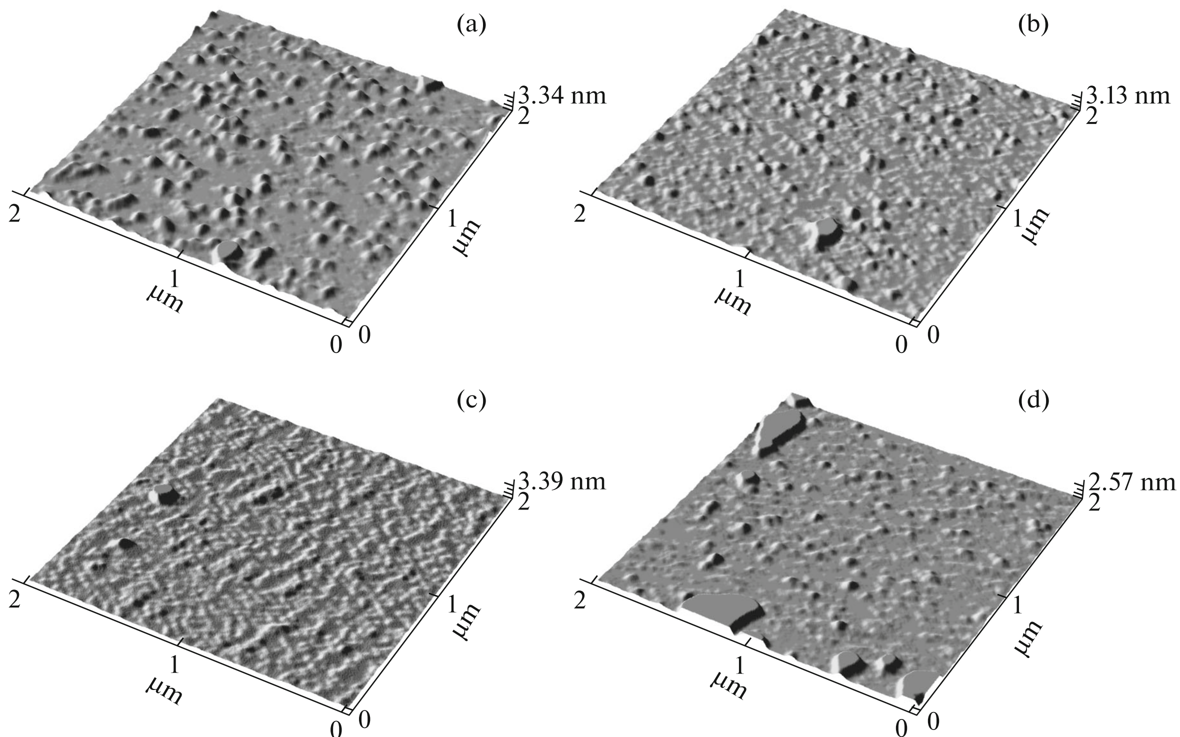

Fig. 3. Surface morphology of the structures with InAs/GaAs QDs: (a) reference structure (R), (b) structure A2 (Mn content is 8×10^{12} cm^{-2}), (c) structure A3 (Mn content is 2×10^{13} cm^{-2}), and (d) structure B3 (Cr content is 8×10^{13} cm^{-2}).

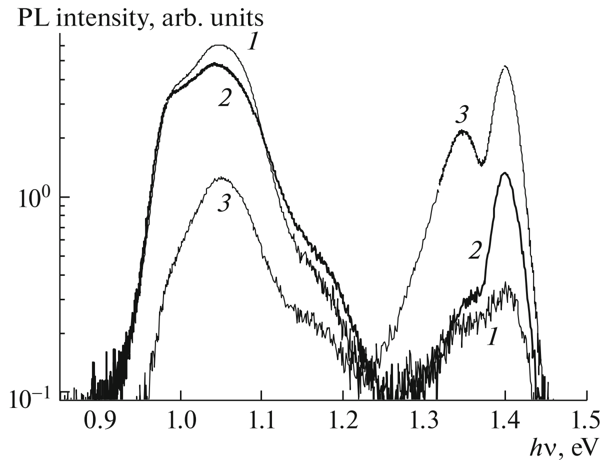

Fig. 4. PL spectra measured for InAs : Cr QDs at 77 K. Cr content is (*1*) 2×10^{13}, (*2*) 4×10^{13}, and (*3*) 8×10^{13} cm^{-2}.

be low (below 5×10^8 cm^{-2}) and it becomes difficult to identify QDs in the AFM micrographs. However, the PL spectra exhibit peaks that can be associated with these clusters (Fig. 2, curve *3*). Together with the change in the clustering thermodynamics, one should mention another important factor: enhanced diffusion mixing of In (from InAs) and Ga (from the substrate) with Mn atoms on the surface [13, 18]. Interdiffusion facilitates the formation of nanoclusters different in composition (InGaAs) that radiate at a shorter wavelength compared to the undoped structures. It was reported [19, 20] that doping by Mn during growth results in the blue shift of the QD luminescence lines. With interdiffusion of In and Ga atoms in mind, the line at 1.4 eV, which is observed in the spectra of the structures with Mn concentrations of 8×10^{12} and 2×10^{13} cm^{-2}, can be assigned to luminescence from $In_xGa_{1-x}As$ solid solution with a variable composition and diffused heterointerface. For example, the formation of a 2D $In_xGa_{1-x}As$ layer by means of diffusion was discussed for QD structures (identical to the reference structures) subjected to high-temperature annealing [21] at 600°C for 30 min.

It is of interest that QDs responsible for radiation at 1 eV are present in all structures (the energy of the corresponding line is exactly the same for all structures). One may infer that the formation of InAs QDs 60/2.5 nm in size is thermodynamically favorable, even in the presence of manganese. The rise in the intensity of the PL line at 1 eV is associated with the general increase in the PL intensity in the presence of manganese atoms. This finding radically distinguishes our QD-based structures from their analogs based on quantum wells (QWs). Manganese introduced into the QW area with a concentration of more than 0.05 at. % completely quenches photoluminescence because of the rise in the rate of nonradiative recombination through Mn impurity levels [22]. Presumably, manganese introduced into the QD structures raises the possibility of nonradiative recombination insignificantly. This may be explained by the fact that the energy level of a hole localized in the QD lies below the energy level of Mn in GaAs. This makes the mechanism of nonradiative recombination through Mn levels in GaAs ineffective at low temperatures (to this end, thermal transfer of the hole from a state in the QD to a Mn level would be required). The general rise in the intensity is associated with the increase in the hole concentration after doping by Mn [10, 11], since it is known that the rate of radiative recombination varies in proportion to the free charge carrier concentration [23].

2.2. Photoluminescence and Surface Morphology of Cr-Doped Structures (Structures B)

The PL spectra of structures B (Fig. 4) exhibit peaks due to radiative transitions between states in the QD. As in the Mn-doped structure, the spectra consist of two PL lines with peaks near 1 and 1.05 eV. Doping by Cr atoms modifies the PL spectrum of the structures (Fig. 4).

(1) The intensity of the second peak grows considerably in comparison with that of the first peak. After doping by Cr with a concentration of 2×10^{13}, 4×10^{13}, and 8×10^{13} cm^{-2} the ratio of the intensity of the second-to-first peak equals 1.50, 1.45, and 2.10, respectively (curves *1*, *2*, and *3*, respectively).

(2) The spectrum contains two additional peaks near 1.35 and 1.40 eV. Their intensity grows with Cr concentration by 22 times. The first-to-fourth peak intensity ratio in structures B1, B2, and B3 equals 12.1, 2.8, and 0.13, respectively.

(3) Compared with the reference structure, the integral intensity of PL from the Cr-doped QDs is higher. With an increase in the Cr concentration, the integral intensity varies as 8.9–8.3–5.4.

(4) AFM studies of the surface morphology of the visualized InAs QD array with a sheet concentration of 8×10^{13} cm^{-2} revealed that the mean size of the QDs remained unchanged compared with the undoped reference structure, whereas the sheet concentration decreased to about 2×10^9 cm^{-2} (Fig. 3d).

Thus, we can conclude that Cr atoms, as well as Mn atoms, present on the surface change the thermodynamic conditions for nanoclustering. In the case of Cr, the size distribution function takes another form. The increase in the second peak of PL compared with the first one is likely to be associated with the redistribution of QDs with different sizes. As follows from the AFM data, the total concentration of QDs (and the relative intensity of PL from QDs) decreases with increasing Cr content (Fig. 4).

The PL peak at 1.4 eV, which is present in the spectra of the Cr-doped QD structures, is likely to be due to radiative transitions in the wetting layer of QDs. The appearance of this peak may indicate increased probability of radiative recombination from the wetting

layer in those areas wherein QDs were not formed. The PL peak at 1.35 eV may be assigned to an array of small QDs that are not visualized during the etching of the cap layer. As the chromium content grows, so does the concentration of small QDs and the corresponding PL peak rises. It should also be noted that the energies 1.35 and 1.40 eV correspond to recombination transitions between defect centers in GaAs [24].

An interesting experimental finding is that the PL intensity remains unchanged or even slightly increases after doping by chromium. Chromium atoms in III–V semiconductors act as deep centers of nonradiative recombination and, when introduced, they usually quench luminescence. However, in the case of our QD structures, no significant decay of luminescence from QDs was observed, except for the structure with the highest chromium content.

CONCLUSIONS

The InAs/GaAs QDs were doped with manganese or chromium during growth. It was shown that doping QD-containing structures by transition elements, one can control the spectral characteristics of PL from these structures, namely, extend the spectral interval and vary the radiation wavelength. Mn(Cr) dopants cause the appearance of high-energy lines in the PL spectra of InAs/GaAs QDs, the intensity of which increases with dopant concentration. Low-energy lines (characteristic of undoped QDs) either persist (but their relative intensity drops) or disappear. The changes in the spectra are presumably associated with the variations in the equilibrium conditions for nanoclustering, which changes the sizes of nanoclusters. Thus, doping by Mn or Cr introduces an extra degree of freedom into the process of technologically controlling the wavelength of radiation from QD structures grown by MOS hydride epitaxy.

ACKNOWLEDGMENTS

The authors thank B.N. Zvonkov for preparing specimens.

This work was supported by the Ministry of Education and Science (project no. 8.1751.2017.PCh), Russian Foundation for Basic Research (grant nos. 15-02-07824, 15-38-20642mol_a_ved, 16-07-01102), and grant no. MK-8221.2016.2) of the President of the Russian Federation).

REFERENCES

1. D. Bimberg and C. Ribbat, Microelectron. J. **34**, 323 (2003).
2. Zh. I. Alferov, Semiconductors **32**, 1 (1998).
3. N. N. Ledentsov, V. M. Ustinov, V. A. Shchukin, P. S. Kop'ev, Zh. I. Alferov, and D. Bimberg, Semiconductors **32**, 343 (1998).
4. D. Bimberg, M. Grundmann, and N. N. Ledentsov, *Quantum Dot Heterostructures* (Wiley, Chichester, 1999).
5. A. E. Zhukov, B. V. Volovik, S. S. Mikhrin, N. A. Maleev, A. F. Tsatsul'nikov, E. V. Nikitina, I. N. Kayander, V. M. Ustinov, and N. N. Ledentsov, Tech. Phys. Lett. **27**, 734 (2001).
6. D. L. Huffaker and D. G. Deppe, Appl. Phys. Lett. **73**, 520 (1998).
7. V. I. Zubkov, C. M. A. Kapteyn, A. V. Solomonov, and D. J. Bimberg, J. Phys.: Condens. Matter **17**, 2435 (2005).
8. B. N. Zvonkov, I. A. Karpovich, N. V. Baidus, D. O. Filatov, S. V. Morozov, and Yu. Yu. Gushina, Nanotecnology **11**, 221 (2000).
9. B. N. Zvonkov, O. V. Vikhrova, Yu. A. Danilov, E. S. Demidov, P. B. Demina, M. V. Dorokhin, Yu. N. Drozdov, V. V. Podol'skii, and M. V. Sapozhnikov, J. Opt. Technol. **75**, 389 (2008).
10. M. Holub, S. Chakrabarti, S. Fathpour, P. Bhattacharya, Y. Lei, and S. Ghosh, Appl. Phys. Lett. **85**, 973 (2004).
11. A. D. Bouravleuv, V. N. Nevedomskii, E. V. Ubyivovk, V. F. Sapega, A. I. Khrebtov, Yu. B. Samsonenko, G. E. Cirlin, and V. M. Ustinov, Semiconductors **47**, 1037 (2013).
12. H. J. Meng, J. Lu, L. Chen, P. F. Xu, J. J. Deng, and J. H. Zhao, Phys. Lett. A **373**, 1379 (2009).
13. M. V. Dorokhin, A. V. Zdoroveishev, E. I. Malysheva, Yu. A. Danilov, B. N. Zvonkov, and A. E. Sholina, J. Surf. Invest.: X-Ray, Synchrotron Neutron Tech. **6**, 511 (2012).
14. I. A. Karpovich, N. V. Baidus, B. N. Zvonkov, S. V. Morozov, D. O. Filatov, and A. V. Zdoroveishev, Nanotecnology **12**, 425 (2001).
15. I. A. Karpovich, A. V. Zdoroveishev, A. P. Gorshkov, D. O. Filatov, and R. N. Skvortsov, Phys. Low-Dimens. Struct. **3/4**, 191 (2003).
16. A. V. Zdoroveishev, Candidate's Dissertation in Mathematics and Physics (Nizhny Novgorod, 2006).
17. S. V. Zaitsev, V. D. Kulakovskii, M. V. Dorokhin, Yu. A. Danilov, P. B. Demina, M. V. Sapozhnikov, O. V. Vikhrova, and B. N. Zvonkov, Phys. E **41**, 652 (2009).
18. M. V. Dorokhin, B. N. Zvonkov, Yu. A. Danilov, V. V. Podolskii, P. B. Demina, O. V. Vikhrova, E. I. Malysheva, and M. V. Sapozhnikov, Int. J. Nanosci. **6**, 221 (2007).
19. Y. K. Zhou, H. Asahi, J. Asakura, S. Okumura, K. Asami, and S. J. Gonda, J. Cryst. Growth **221**, 605 (2000).
20. S. Nagahara, S. Tsukamoto, and Y. J. Arakawa, J Cryst. Growth **301–302**, 797 (2007).
21. A. V. Zdoroveishev, M. V. Dorokhin, E. I. Malysheva, and P. B. Demina, in *Innovation Technologies*, Ed. by S. V. Bulyarskii (Ul'yanovsk. Gos. Univ., Ul'yanovsk, 2010), Vol. 3, p. 84.
22. M. Poggio, R. C. Myers, N. P. Stern, A. C. Gossard, and D. D. Awschalom, Phys. Rev. B **72**, 235313 (2005).
23. E. F. Schubert, *Light-Emitting Diodes* (Cambridge Univ. Press, 2006).
24. L. Pavesi and M. Guzzi, J. Appl. Phys. **75**, 4779 (1994).

Translated by V. Isaakyan